

NGU Report 2014.039

Helicopter-borne magnetic, electromagnetic and  
radiometric geophysical survey at Northern  
Senja in 2012, 2013 and 2014,  
Troms County.

Report no.: 2014.039		ISSN 0800-3416	Grading: Open
Title: Helicopter-borne magnetic, electromagnetic and radiometric geophysical survey at Northern Senja in 2012, 2013 and 2014, Troms County.			
Authors: : Alexei Rodionov, Frode Ofstad, Alexandros Stampolidis & Georgios Tassis.		Client: NGU	
County: Troms		Municipalities: Berg, Lenvik and Tranøy	
Map-sheet name (M=1:250.000) TROMSO		Map-sheet no. and -name (M=1:50.000) 1333 I Stonglandet, 1433 I Lenvik, 1433 II Tranøy 1433 IV Melfjordbotn, 1434 III Hekkingen	
Deposit name and grid-reference: Senja UTM 33 W 604000 – 7700000		Number of pages: 32 Price (NOK): 120,- Map enclosures:	
Fieldwork carried out: July-August 2012, August 2013, September 2014	Date of report: October 22 <sup>nd</sup> 2014	Project no.: 342900	Person responsible: <i>Jan S. Rønning</i>
<p>Summary:</p> <p>As a part of the MINN project, NGU conducted an airborne geophysical survey at Senja in July-August 2012 and August 2013 (Rodionov et al. 2013). For special reasons, a small area were not measured until September 2014. This report describes and documents the acquisition, processing and visualization of <b>all recorded datasets from Senja</b>. The geophysical survey results reported herein are 5620 line km, covering an area of 1124 km<sup>2</sup>.</p> <p>The NGU modified Geotech Ltd. Hummingbird frequency domain system supplemented by optically pumped Cesium magnetometer and 1024 channels RSX-5 spectrometer was used for data acquisition.</p> <p>The main part of the survey was flown with 200 m line spacing and lines were oriented at a 55° azimuth in UTM zone 33 W coordinates. The northern part of the survey area was flown with 200 m line spacing and line orientation at 145° due to the extreme rugged terrain. The area around the Skaland and the Trælen graphite mines was flown with 100 m line spacing and line oriented at 125°-160° azimuth.</p> <p>Collected data were processed at NGU using Geosoft Oasis Montaj software. Raw total magnetic field data were corrected for diurnal variation and levelled using standard micro levelling algorithm. EM data were filtered and levelled using both automated and manual levelling procedure. Apparent resistivity was calculated from in-phase and quadrature data for each of the five frequencies separately using a homogeneous half space model. Apparent resistivity grids were filtered using 3x3 convolution filter.</p> <p>Radiometric data were processed using standard procedures recommended by International Atomic Energy Association.</p> <p>Data were gridded with the cell size of 50 x 50 m and presented as a shaded relief maps at the scale of 1:50 000.</p>			
Keywords: Geophysics	Airborne	Magnetic	
Electromagnetic	Gamma spectrometry	Radiometric	
		Technical report	

## Table of Contents

1. INTRODUCTION .....	4
2. SURVEY SPECIFICATIONS .....	5
2.1 Airborne Survey Parameters.....	5
2.2 Airborne Survey Instrumentation .....	6
2.3 Airborne Survey Logistics Summary .....	7
3. DATA PROCESSING AND PRESENTATION .....	7
3.1 Total Field Magnetic Data .....	7
3.2 Electromagnetic Data .....	9
3.3 Radiometric data .....	10
4. PRODUCTS.....	14
5. REFERENCES .....	15
Appendix A1: Flow chart of magnetic processing.....	16
Appendix A2: Flow chart of EM processing.....	16
Appendix A3: Flow chart of radiometry processing.....	16

## FIGURES

Figure 1: Senja survey area.....	4
Figure 2: Hummingbird system in air .....	7
Figure 3: An example of Gamma-ray spectrum showing the position of the K, Th, U and Total count windows. ....	11
Figure 3: Senja survey area with flight path .....	20
Figure 4: Total Magnetic Field .....	21
Figure 5: Magnetic Vertical Derivative.....	22
Figure 6: Magnetic Tilt Derivative .....	23
Figure 7: Apparent resistivity. Frequency 34000 Hz, Coplanar coils .....	24
Figure 8: Apparent resistivity. Frequency 6600 Hz, Coplanar coils .....	25
Figure 9: Apparent resistivity. Frequency 880 Hz, coplanar coils .....	26
Figure 10: Apparent resistivity. Frequency 7000 Hz, Coaxial coils .....	27
Figure 11: In-phase and quadrature responses. Frequency 980 Hz, Coaxial coils .....	28
Figure 12: Uranium ground concentration.....	29
Figure 13: Thorium ground concentration .....	30
Figure 14: Potassium ground concentration.....	31
Figure 15: Radiometric Ternary map .....	32

## TABLES

Table 1. Instrument Specifications .....	6
Table 2. Hummingbird electromagnetic system, frequency and coil configurations.....	6
Table 3: Specified channel windows for the 1024 RSX-5 systems used in this survey ....	11
Table 4: Maps in scale 1:50000 available from NGU on request.....	14

## 1. INTRODUCTION

In 2011 the Norwegian government initiated a new program for mapping of mineral resources in Northern Norway (MINN). The goal of this program is to enhance the geological information that is relevant to an assessment of the mineral potential of the three northernmost counties. The airborne geophysical surveys - helicopter borne and fixed wing- are important integral part of MINN program. The airborne survey results reported herein amount to 5620 line km (1124 km<sup>2</sup>) over the Northern Senja, as shown in Figure 1.



**Figure 1: Senja survey area**

The objective of the airborne geophysical survey was to obtain a dense high-resolution aeromagnetic, electromagnetic and radiometric data over the survey area. This data is required for the enhancement of a general understanding of the regional geology of the area. In this regard, the data can also be used to map contacts and structural features within the property. It also improves defining the potential of known zones of mineralization, their geological settings, and identifying new areas of interest.

The survey incorporated the use of a Hummingbird™ five-frequency electromagnetic system supplemented by a high-sensitivity caesium magnetometer, gamma-ray spectrometer and radar altimeter. A GPS navigation computer system with flight path indicators ensured accurate positioning of the geophysical data with respect to the World Geodetic System 1984 geodetic datum (WGS-84).

EM data from part of this survey, in The Skaland –Trælen mining area, are inverted and pseudo 3D images of graphite mineralisations are presented (Rønning et al. 2012).

## 2. SURVEY SPECIFICATIONS

### 2.1 Airborne Survey Parameters

NGU used a Hummingbird™ electromagnetic and magnetic helicopter survey system designed to obtain low level, slow speed, detailed airborne magnetic and electromagnetic data (Geotech 1997). The system was supplemented by 1024 channel gamma-ray spectrometer which was used to map ground concentrations of U, Th and K.

The airborne survey began on July 31st and suspended on August 19th, 2012. The survey was continued on August 9 and suspended again on August 23, 2013 due to local restrictions. Finally, the last portion of the area was covered by survey on September 18, 2014. A Eurocopter AS350-B3 helicopter from helicopter company HeliScan AS was used to tow the bird. The main part of the survey was flown with 200 m line spacing and lines were oriented at a 55° azimuth in UTM zone 33 W coordinates. The northern part of the survey area was flown with 200 m line spacing and line orientation at 145° due to the extreme rugged terrain. The area around the Skaland and the Trælen graphite mines was flown with 100 m line spacing and line oriented at 125°-160° azimuth. This part of the survey was partly financed by Skaland Graphite as and previously reported (Rønning et al. 2012). The line paths at the Senja survey is shown in figure 3.

The magnetic and electromagnetic sensors are housed in a single 7.5 m long bird, which was maintained at an average of 60 m above the topographic surface. A gamma-ray spectrometer installed under the belly of the helicopter registered natural gamma ray radiation simultaneously with the acquisition of magnetic/EM data.

Just before the start of 2014 field season, instrumental problems were discovered. The highest frequency (34 kHz) was not stable, and this instability influenced on the quality of the other frequencies. To be able to collect high quality data for the four lowest frequencies, it was decided not to transmit on 34 kHz.

Rugged terrain and abrupt changes in topography affected the aircraft pilot's ability to 'drape' the terrain; therefore the average instrumental height was much higher than the standard survey instrumental height, which is defined as 30 m plus a height of obstacles (trees, power lines etc.).

The ground speed of the aircraft varied from 50 – 130 km/h depending on topography, wind direction and its magnitude. On average the ground speed during measurements is calculated to 65 km/h. Magnetic data were recorded at 0.2 second intervals resulting in approximately 4 m observation point spacing. EM data were recorded at 0.1 second intervals resulting in data with a sample increment of ~2 m along the ground in average. Spectrometry data were recorded every 1 second giving a point spacing of approximately 18 meter. The above parameters are sufficient to obtain details in the data to detect subtle anomalies that may represent mineralization and/or rocks of different lithological and petrophysical composition

The base magnetometers to monitor diurnal variations in the magnetic field, was located at Finnsnes just outside the measured area for the eastern part of the survey and at Skaland inside the measured area for the western part. Two magnetometers were used as magnetic base stations. Scintrex Envi-Mag recorded every 3 second was used during 2012 year survey. The CPU clock of the base magnetometer computer was synchronized to the CPU clock of the DAS on a daily basis. Gem GSM-19 station magnetometer was used during 2013 year survey

and its data were recorded once every 1 second in 2013 and 3 second during 2014 year survey. The CPU clock of the base magnetometer and the helicopter magnetometer were both synchronized to GMT (Greenwich Mean Time) through the built-in GPS receiver to allow correction of diurnals.

Navigation system uses GPS/GLONASS satellite tracking systems to provide real-time WGS-84 coordinate locations for every second. The accuracy achieved with no differential corrections is reported to be  $\pm 5$  m in the horizontal directions. The GPS receiver antenna was mounted externally to the tail tip of the helicopter.

For quality control, the electromagnetic, magnetic and radiometric, altitude and navigation data were monitored on four separate windows in the operator's display during flight while they were recorded in three data ASCII streams to the PC hard disk drive. Spectrometry data were also recorded to an internal hard drive of the spectrometer. The data files were transferred to the field workstation via USB flash drive. The raw data files were backed up onto USB flash drive in the field.

## 2.2 Airborne Survey Instrumentation

Instrument specification is given in **Table 1**. Frequencies and coil configuration for the Hummingbird EM system is given in **Table 2**.

**Table 1. Instrument Specifications**

Instrument	Producer/Model	Accuracy	Sampling frequency
Magnetometer	Scintrex Cs-2	0,002 nT	5 Hz (2013)
Base magnetometer	Scintrex Envi GEM GSM-19	0.1 nT 0.1 nT	3 sec (2012) 1 sec (2013) 3 sec (2014)
Electromagnetic	Geotech Hummingbird	1 – 2 ppm	10 Hz
Gamma spectrometer	Radiation Solutions RSX-5	1024 ch's, 16 liters down, 4 liters up	1 Hz
Radar altimeter	Bendix/King KRA 405B	$\pm 3\%$ 0 – 500 fot $\pm 5\%$ 500 – 2500 fot	1 Hz
Pressure/temperature	Honeywell PPT	$\pm 0,03\%$ FS	1 Hz
Navigation	Topcon GPS-receiver	$\pm 5$ meter	1 Hz
Acquisition system	PC based in house software		

**Table 2. Hummingbird electromagnetic system, frequency and coil configurations**

Coils:	Frequency	Orientation	Separation
A	7700 Hz	Coaxial	6.20 m
B	6600 Hz	Coplanar	6.20 m
C	980 Hz	Coaxial	6.025 m
D	880 Hz	Coplanar	6.025 m
E	34000 Hz	Coplanar	4.87 m

## 2.3 Airborne Survey Logistics Summary

Traverse (survey) line spacing: 200 metres  
Traverse line spacing (Northern part): 100 and 200m  
Traverse line direction (Southern part): 55° SE-NW  
Traverse line direction (Northern part): 125°-160° NW-SE  
Nominal aircraft ground speed: 50 - 130 km/h  
Average sensor terrain clearance EM+Mag: 60 metres  
Average sensor terrain clearance Rad: 90 metres  
Sampling rates:       0.1-0.2 seconds - magnetometer  
                          0.1 seconds - electromagnetics  
                          1.0 second - spectrometer, GPS, altimeter



Figure 2: Hummingbird system in air

## 3. DATA PROCESSING AND PRESENTATION

All data were processed by Alexei Rodionov (AR Geoconsulting Ltd., Canada) in Calgary. The ASCII data files were loaded into three separate Oasis Montaj databases. All three datasets were processed consequently according to processing flow charts shown in Appendix A1, A2 and A3.

### 3.1 Total Field Magnetic Data

At the first stage the raw magnetic data were visually inspected and spikes were removed manually. Non-linear filter was also applied to airborne raw data to eliminate short-period spikes.

Typically, several corrections have to be applied to magnetic data before gridding - heading correction, lag correction and diurnal correction.

### Diurnal Corrections

The temporal fluctuations in the magnetic field of the earth affect the total magnetic field readings recorded during the airborne survey. This is commonly referred to as the magnetic diurnal variation. These fluctuations can be effectively removed from the airborne magnetic dataset by using a stationary reference magnetometer that records the magnetic field of the earth simultaneously with the airborne sensor at given short time interval. The data from base station were imported in database using the standard Oasis magbase.gx module. Diurnal variation channel was inspected for spikes and spikes were removed manually if necessary. Magnetic diurnals data were within the standard NGU specifications during the entire survey (Rønning 2013).

Diurnal variations were measured with GEM GSM-19 and Scintrex Envi magnetometers (2012). The recorded data are merged with the airborne data and the diurnal correction is applied according to equation (1).

$$\mathbf{B}_{Tc} = \mathbf{B}_T + (\bar{\mathbf{B}}_B - \mathbf{B}_B), \quad (1)$$

where:

$\mathbf{B}_{Tc}$  = Corrected airborne total field readings

$\mathbf{B}_T$  = Airborne total field readings

$\bar{\mathbf{B}}_B$  = Average datum base level

$\mathbf{B}_B$  = Base station readings

### Corrections for Lag and heading

Neither a lag nor cloverleaf tests were performed before the survey. According to previous reports the lag between logged magnetic data and the corresponding navigational data was 1-2 fids. Translated to a distance it would be no more than 10 m - the value comparable with the precision of GPS. A heading error for a towed system is usually either very small or non-existent. So no lag and heading corrections were applied.

### Magnetic data processing, gridding and presentation

The total field magnetic anomaly data ( $\mathbf{B}_{TA}$ ) were calculated from the diurnal corrected data ( $\mathbf{B}_{Tc}$ ) after subtracting the IGRF for the surveyed area calculated for the data period (eq.2)

$$\mathbf{B}_{TA} = \mathbf{B}_{Tc} - IGRF \quad (2)$$

The total field anomaly data were gridded using a minimum curvature method with a grid cell size of 50 meters. This cell size is equal to one quarter of the 200 m average line spacing. In order to remove small line-to-line levelling errors that were detected on the gridded magnetic anomaly data, the Geosoft Micro-levelling technique was applied on the flight line based magnetic database. Then, the micro-levelled channel was gridded using again a minimum curvature method with 50 m grid cell size. Finally, 3x3 convolution filter was applied to smooth the grid.

Note. Part of magnetic data from flight 36, lines 1870-1940 was lost due to problems with bird electronics and data were interpolated.

The processing steps of magnetic data presented so far, were performed on point basis. The following steps are performed on grid basis. Vertical Gradient along with the Tilt Derivative of the total magnetic anomaly were calculated from the micro-levelled total magnetic anomaly grid. The Tilt derivative (TD) was calculated according to the equation (3)

$$TD = \tan^{-1} \left( \frac{VG}{HG} \right) \quad (3)$$

The results are presented in coloured shaded relief maps:

- A. Total field magnetic anomaly
- B. Vertical gradient of total magnetic anomaly
- C. Tilt angle (or Tilt Derivative) of the total magnetic anomaly
- D.

These maps are representative of the distribution of magnetization over the surveyed areas. The list of the produced maps is shown in Feil! Fant ikke referansebildene..

### **3.2 Electromagnetic Data**

The DAS computer records both an in-phase and a quadrature value for each of the five coil sets of the electromagnetic system. Instrumental noise and drift should be removed before computation of an apparent resistivity.

#### **Instrumental noise**

In-phase and quadrature data were filtered with 3-5 fids non-linear filter to eliminate spheric spikes which were represented as irregular spikes of large amplitude in records. Simultaneously, the 30 -120 fids low-pass filter was also applied to suppress instrumental and cultural noise. Due to problems in electronics of EM system in 2013, the internal noise was higher than standard 1-2 pmm and reached 3-5 ppm on 880, 980, 6600 HZ in-phase and quadrature data and up to 15 ppm on 34000 Hz . Low pass filter was not able to suppress the noise completely due to irregular nature of noise and the quality of data is suffered partly from low signal/noise ratio.

#### **Instrument Drift**

In order to remove the effects of instrument drift caused by gradual temperature variations in the transmitting and receiving circuits, background responses are recorded during each flight. To obtain a background level the bird is raised to an altitude of approximately 1000 ft above the topographic surface so that no electromagnetic responses from the ground are present in the recorded traces. The EM traces observed at this altitude correspond to a background (zero) level of the system. If these background levels are recorded at 20-30 minute intervals, then the drift of the system (assumed to be linear) can be removed from the data by resetting these points to the initial zero level of the system. The drift must be removed on a flight-by-flight basis, before any further processing is carried out. Geosoft HEM module was used for applying drift correction. Residual instrumental drift, usually small, but often non-linear, was manually removed on line-to-line basis.

### **Apparent resistivity calculation and presentation**

When levelling of the EM data was complete, apparent resistivity was calculated from in-phase and quadrature EM components using a homogeneous half space model of the Earth (Geosoft HEM module) for all five frequencies. Threshold of 3 ppm was set for inversion of 34000 Hz data, 2 ppm for 6600, 7000, 880 and 1 ppm for 980 Hz. Due to low signal/noise ratio, the resolution of EM survey in high resistivity area was also very low that is especially noticeable on 880 and 980 Hz resistivity maps.

Secondary electromagnetic field decays rapidly with the distance (height of the sensors) – as  $z^{-2} - z^{-5}$  depending on the shape of the conductors and, at certain height, signals from the ground sources become comparable with instrumental noise. Levelling errors or precision of levelling can lead sometimes to appearance of artificial resistivity anomalies when data were collected at high instrumental altitude. Application of threshold allows excluding such data from an apparent resistivity calculation, though not completely. It's particularly noticeable in low frequencies datasets. Resistivity data were visually inspected; artificial anomalies associated with high altitude measurements were manually removed.

Data, recorded at the height above 100 m were considered as non-reliable and removed from gridding. Remaining resistivity data were gridded with a cell size 50 m and 3x3 convolution filter was applied to smooth resistivity grids.

Note 1. Part of EM data from flight 36, lines 1910-1940 (western corner) are absent due to problems with bird electronics.

Note 2. Due to problems with 34 kHz channel in 2014, the gap on resistivity map in central part of the survey area remained uncovered.

### **3.3 Radiometric data**

Airborne gamma-ray spectrometry measures the abundance of Potassium (K), Thorium (eTh), and Uranium (eU) in rocks and weathered materials by detecting gamma-rays emitted due to the natural radioelement decay of these elements. The data analysis method is based on the IAEA recommended method for U, Th and K (International Atomic Energy Agency, 1991; 2003). A short description of the individual processing steps of that methodology as adopted by NGU is given bellow:

#### **Energy windows**

The Gamma-ray spectra were initially reduced into standard energy windows corresponding to the individual radio-nuclides K, U and Th.

**Figure 3** shows an example of a Gamma-ray spectrum and the corresponding energy windows and radioisotopes (with peak energy in MeV) responsible for the radiation.

The RSX-5 is a 1024 channel system with four downward and one upward looking detectors and the actual Gamma-ray spectrum is divided into 1024 channels. The first channel is reserved for the "Live Time" and the last for the Cosmic rays. **Table 3** shows the channels that were used for the reduction of the spectrum.

Table 3: Specified channel windows for the 1024 RSX-5 systems used in this survey

Gamma-ray spectrum	Cosmic	Total count	K	U	Th
Down	1022	134-934	454-521	551-617	801-934
Up	1022			551-617	
Energy windows (MeV)	>3.07	0.41-2.81	1.37-1.57	1.66-1.86	2.41-2.81

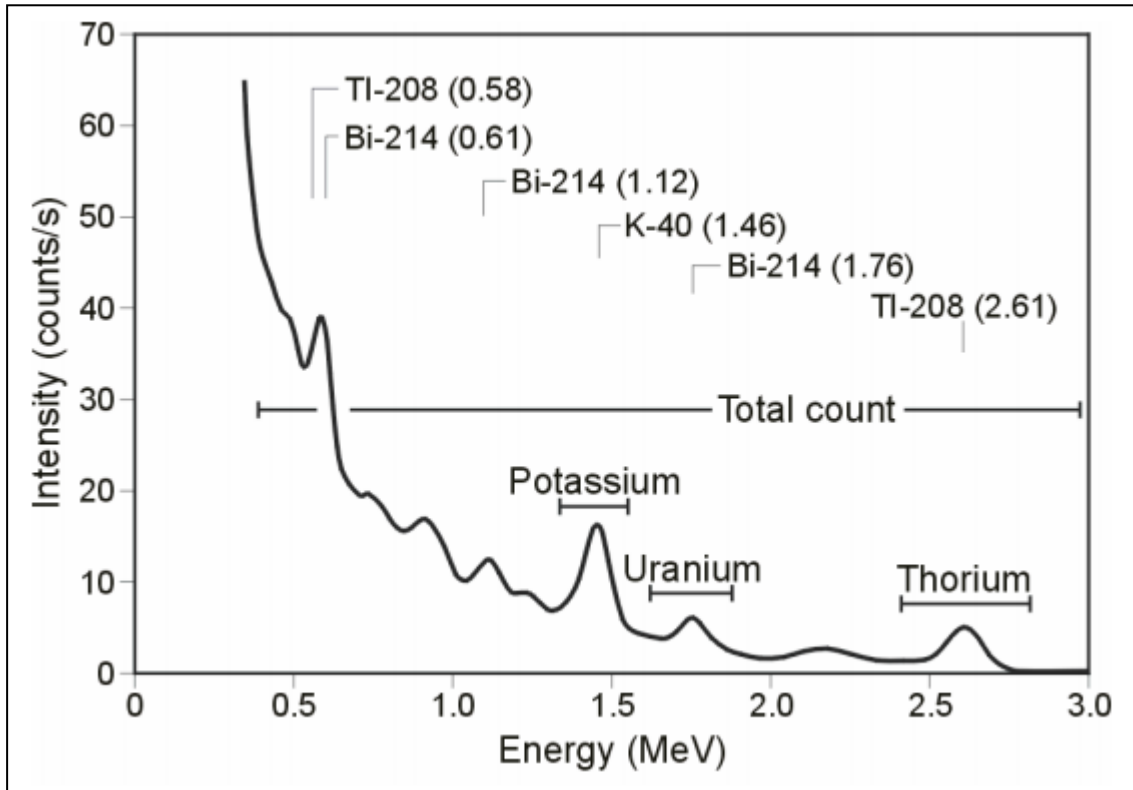


Figure 3: An example of Gamma-ray spectrum showing the position of the K, Th, U and Total count windows.

#### Live Time correction

The data were corrected for live time. “Live time” is an expression of the relative period of time the instrument was able to register new pulses per sample interval. On the other hand “dead time” is an expression of the relative period of time the system was unable to register new pulses per sample interval. The relation between “dead” and “live time” is given by the equation (4)

$$\text{“Live time”} = \text{“Real time”} - \text{“Dead time”} \quad (4)$$

where the “real time” or “acquisition time” is the elapsed time over which the spectrum is accumulated (1 second).

The live time correction is applied to the total count, Potassium, Uranium, Thorium, upward Uranium and cosmic channels. The formula used to apply the correction is as follows:

$$C_{LT} = C_{RAW} \cdot \frac{1000000}{Live\ Time} \quad (5)$$

where  $C_{LT}$  is the live time corrected channel in counts per second,  $C_{RAW}$  is the raw channel data in counts per second and Live Time is in microseconds.

### Cosmic and aircraft correction

Background radiation resulting from cosmic rays and aircraft contamination was removed from the total count, Potassium, Uranium, Thorium, upward Uranium channels using the following formula:

$$C_{CA} = C_{LT} - (a_c + b_c \cdot C_{Cos}) \quad (6)$$

where  $C_{CA}$  is the cosmic and aircraft corrected channel,  $C_{LT}$  is the live time corrected channel  $a_c$  is the aircraft background for this channel,  $b_c$  is the cosmic stripping coefficient for this channel and  $C_{Cos}$  is the low pass filtered cosmic channel.

### Radon correction

The upward detector method, as discussed in IAEA (1991), was applied to remove the effects of the atmospheric radon in the air below and around the helicopter. Usages of over-water measurements where there is no contribution from the ground, enabled the calculation of the coefficients ( $a_C$  and  $b_C$ ) of the linear equations that relate the cosmic corrected counts per second of Uranium channel with total count, Potassium, Thorium and Uranium upward channels over water. Data over-land was used in conjunction with data over-water to calculate the  $a_1$  and  $a_2$  coefficients used in equation (7) for the determination of the Radon component in the downward uranium window:

$$Radon_U = \frac{U_{up_{CA}} - a_1 \cdot U_{CA} - a_2 \cdot Th_{CA} + a_2 \cdot b_{Th} - b_U}{a_U - a_1 - a_2 \cdot a_{Th}} \quad (7)$$

where  $Radon_u$  is the radon component in the downward uranium window,  $U_{up_{CA}}$  is the filtered upward uranium,  $U_{CA}$  is the filtered Uranium,  $Th_{CA}$  is the filtered Thorium,  $a_1$ ,  $a_2$ ,  $a_U$  and  $a_{Th}$  are proportional factors and  $b_U$  and  $b_{Th}$  are constants determined experimentally.

The effects of Radon in the downward Uranium are removed by simply subtracting  $Radon_U$  from  $U_{CA}$ . The effects of radon in the other channels are removed using the following formula:

$$C_{RC} = C_{CA} - (a_C \cdot Radon_U + b_C) \quad (8)$$

where  $C_{RC}$  is the Radon corrected channel,  $C_{CA}$  is the cosmic and aircraft corrected channel,  $Radon_U$  is the Radon component in the downward uranium window,  $a_C$  is the proportionality factor and  $b_C$  is the constant determined experimentally for this channel from over-water data.

### Compton Stripping

Potassium, Uranium and Thorium Radon corrected channels, are subjected to spectral overlap correction. Compton scattered gamma rays in the radio-nuclides energy windows were corrected by window stripping using Compton stripping coefficients determined from measurements on calibrations pads at the Geological Survey of Norway in Trondheim (for values, see Appendix A3).

The stripping corrections are given by the following formulas:

$$A_1 = 1 - (g \cdot \gamma) - (a \cdot \alpha) + (a \cdot g \cdot \beta) - (b \cdot \beta) + (b \cdot \alpha \cdot \gamma) \quad (9)$$

$$U_{ST} = \frac{Th_{RC} \cdot ((g \cdot \beta) - \alpha) + U_{RC} \cdot (1 - b \cdot \beta) + K_{RC} \cdot ((b \cdot \alpha) - g)}{A_1} \quad (10)$$

$$Th_{ST} = \frac{Th_{RC} \cdot (1 - (g \cdot \gamma)) + U_{RC} \cdot (b \cdot \gamma - a) + K_{RC} \cdot ((a \cdot g) - b)}{A_1} \quad (11)$$

$$K_{ST} = \frac{Th_{RC} \cdot ((\alpha \cdot \gamma) - \beta) + U_{RC} \cdot ((a \cdot \beta) - \gamma) + K_{RC} \cdot (1 - (a \cdot \alpha))}{A_1} \quad (12)$$

where  $U_{RC}$ ,  $Th_{RC}$ ,  $K_{RC}$  are the radon corrected Uranium, Thorium and Potassium and  $a$ ,  $b$ ,  $g$ ,  $\alpha$ ,  $\beta$ ,  $\gamma$  are Compton stripping coefficients.

### Reduction to Standard Temperature and Pressure

The radar altimeter data were converted to effective height ( $H_{STP}$ ) using the acquired temperature and pressure data, according to the expression:

$$H_{STP} = H \cdot \frac{273.15}{T + 273.15} \cdot \frac{P}{1013.25} \quad (13)$$

where  $H$  is the smoothed observed radar altitude in meters,  $T$  is the measured air temperature in degrees Celsius and  $P$  is the measured barometric pressure in millibars.

### Height correction

Variations caused by changes in the aircraft altitude relative to the ground was corrected to a nominal height of 60 m. Data recorded at the height above 150 m were considered as non-reliable and removed from processing. Total count, Uranium, Thorium and Potassium stripped channels were subjected to height correction according to the equation:

$$C_{60m} = C_{ST} \cdot e^{C_{ht}(60-H_{STP})} \quad (14)$$

where  $C_{ST}$  is the stripped corrected channel,  $C_{ht}$  is the height attenuation factor for that channel and  $H_{STP}$  is the effective height.

### Conversion to ground concentrations

Finally, corrected count rates were converted to effective ground element concentrations using calibration values derived from calibration pads at the Geological Survey of Norway in Trondheim (for values, see Appendix A3). The corrected data provide an estimate of the apparent surface concentrations of Potassium, Uranium and Thorium ( $K$ ,  $eU$  and  $eTh$ ). Potassium concentration is expressed as a percentage, equivalent Uranium and Thorium as parts per million (ppm). Uranium and Thorium are described as “equivalent” since their presence is inferred from gamma-ray radiation from daughter elements ( $^{214}Bi$  for Uranium,  $^{208}Tl$  for Thorium). The concentration of the elements is calculated according to the following expressions:

$$C_{CONC} = C_{60m} / C_{SENS\_60m} \quad (15)$$

where  $C_{60m}$  is the height corrected channel,  $C_{SENS\_60m}$  is experimentally determined sensitivity reduced to the nominal height (60m).

### **Spectrometry data gridding and presentation**

Gamma-rays from Potassium, Thorium and Uranium emanate from the uppermost 30 to 40 centimetres of soil and rocks in the crust (Minty, 1997). Variations in the concentrations of these radioelements largely related to changes in the mineralogy and geochemistry of the Earth's surface.

The spectrometry data were stored in a database and the ground concentrations were calculated following the processing steps. A list of the parameters used in these steps is given in Appendix A3.

Then the data were split in lines and ground concentrations of the three main natural radioelements Potassium, Thorium and Uranium and total gamma-ray flux (total count) were gridded using a minimum curvature method with a grid cell size of 50 meters. In order to remove small line-to-line levelling errors appeared on those grids, the data were micro-levelled as in the case of the magnetic data, and re-gridded with the same grid cell size. Finally, a 3x3 convolution filter was applied to Uranium grid to smooth the microlevelled concentration grids.

Quality of the radiometric data was within standard NGU specifications (Rønning 2013). For further reading regarding standard processing of airborne radiometric data, we recommend the publications from Minty et al. (1997).

## **4. PRODUCTS**

Processed digital data from the survey are presented as:

1. Three Geosoft XYZ files:  
Senja\_Mag\_2014.xyz, Senja\_EM\_2014.xyz, Senja\_Rad\_2014.xyz
2. Coloured maps (jpg) at the scale 1:50000 available from NGU on request
3. Georeferenced tiff-files (Geo-Tiff).

**Table 4: Maps in scale 1:50000 available from NGU on request.**

Map #	Name
2014.039-01	Total magnetic field
2014.039-02	Magnetic Vertical Derivative
2014.039-03	Magnetic Tilt Derivative
2014.039-04	Apparent resistivity, Frequency 34000 Hz, coplanar coils
2014.039-05	Apparent resistivity, Frequency 6600 Hz, coplanar coils
2014.039-06	Apparent resistivity, Frequency 880 Hz, coplanar coils
2014.039-07	Apparent resistivity, Frequency 7000 Hz, coaxial coils
2014.039-08	Apparent resistivity, Frequency 980 Hz, coaxial coils
2014.039-09	Uranium ground concentration
2014.039-10	Thorium ground concentration
2014.039-11	Potassium ground concentration
2014.039-12	Radiometric Ternary Map

Downscaled images of the maps are shown on figures 4 to 15. Data and maps are available from [www.ngu.no](http://www.ngu.no).

## 5. REFERENCES

- Geotech 1997: Hummingbird Electromagnetic System. User manual. Geotech Ltd. October 1997
- Grasty, R.L., Holman, P.B. & Blanchard 1991: Transportable Calibration pads for ground and airborne Gamma-ray Spectrometers. Geological Survey of Canada. Paper 90-23. 62 pp.
- IAEA 2003: Guidelines for radioelement mapping using gamma ray spectrometry data. IAEA-TECDOC-1363, Vienna, Austria. 173 pp.
- Minty, B.R.S., Luyendyk, A.P.J. and Brodie, R.C. 1997: Calibration and data processing for gamma-ray spectrometry. AGSO – Journal of Australian Geology & Geophysics. 17(2). 51-62.
- Naudy, H. and Dreyer, H. 1968: Non-linear filtering applied to aeromagnetic profiles. Geophysical Prospecting. 16(2). 171-178.
- Rodionov, A., Ofstad, F., Stamoplidis, A., & R`Tassis, G. 2013: Helicopterborne magnetic, electromagnetic and radiometric geophysical survey in the Senja area, Berg, Lenvik, and Tranøy Municipalities, Troms County. NGU Report 2013.047, 26 pp.
- Rønning, J.S., Rodionov, A., Ofstad, F. og Lynum, R. 2012: Elektromagnetiske, magnetiske, og radiometriske målinger fra helikopter i området Skaland - Trælen på Senja. NGU Rapport 2012.061 (30s.).
- Rønning, J.S. 2013: NGUs helikoptermålinger. Plan for sikring og kontroll av datakvalitet. NGU Intern rapport 2013.001, (38 sider).

## Appendix A1: Flow chart of magnetic processing

Meaning of parameters is described in the referenced literature.

Processing flow:

- Quality control.
- Visual inspection of airborne data and manual spike removal
- Import magbase data to Geosoft database
- Inspection of magbase data and removal of spikes
- Correction of data for diurnal variation
- Splitting flight data by lines
- Gridding
- Microlevelling
- 3x3 convolution filter

## Appendix A2: Flow chart of EM processing

Meaning of parameters is described in the referenced literature.

Processing flow:

- Filtering of in-phase and quadrature channels with low pass filters
- Automated leveling
- Quality control
- Visual inspection of data.
- Splitting flight data by lines
- Manual removal of remaining part of instrumental drift
- Calculation of an apparent resistivity using both - in-phase and quadrature channels
- Gridding
- 3x3 convolution filter

## Appendix A3: Flow chart of radiometry processing

Underlined processing stages are not only applied to the K, U and Th window, but also to the total. Meaning of parameters is described in the referenced literature.

**Processing flow:**

- **Quality control**
- **Airborne and cosmic correction (IAEA, 2003)**

**2012 survey data**

Used parameters: (determined by high altitude calibration flights near Seljord in June 2012)

Aircraft background counts:

K window	7
U window	2
Th window	0
Uup window	0
Total counts	44

Cosmic background counts (normalized to unit counts in the cosmic window):

K window	0.0701
U window	0.0463
Uup window	0.0505
Th window	0.0664
Total counts	1.1228

### 2013 survey data

Used parameters: (determined by high altitude calibration flights near Langoya in July 2013)

Aircraft background counts:

K window 7  
U window 0.9  
Th window 0.9  
Uup window 0  
Total counts 36

Cosmic background counts (normalized to unit counts in the cosmic window):

K window 0.0617  
U window 0.0454  
Uup window 0.0423  
Th window 0.0647  
Total counts 1.0379

### 2014 survey data

Used parameters: (determined by high altitude calibration flights near Frosta in January 2014)

Aircraft background counts:

K window 5.3584  
U window 1.427  
Th window 0  
Uup window 0.7051  
Total counts 42

Cosmic background counts (normalized to unit counts in the cosmic window):

K window 0.057  
U window 0.0467  
Uup window 0.0448  
Th window 0.0643  
Total counts 1.0317

- **Radon correction using upward detector method (IAEA, 2003)**

#### 2012 survey data:

Used parameters (determined from survey data over water and land):

$a_u$ : 0.342       $b_u$ : 0.6339  
 $a_K$ : 0.989       $b_K$ : 1.4306  
 $a_T$ : 0.0605       $b_T$ : 0.5425  
 $a_{Tc}$ : 19.449       $b_{Tc}$ : -3.6222  
 $a_1$ : 0.01320       $a_2$ : 0.05054

#### 2013 survey data

Used parameters (determined from survey data over water and land):

$a_u$ : 0.3048       $b_u$ : 0.5941  
 $a_K$ : 0.9525       $b_K$ : 2.2398  
 $a_T$ : 0.0635       $b_T$ : 0.2371  
 $a_{Tc}$ : 16.119       $b_{Tc}$ : 8.0586  
 $a_1$ : 0.01320       $a_2$ : 0.05054

#### 2014 survey data

Used parameters (determined from survey data over water and land):

$a_u$ : 0.3681       $b_u$ : 0.1763  
 $a_K$ : 0.8101       $b_K$ : 0.3044  
 $a_T$ : 0.1317       $b_T$ : 0.6278  
 $a_{Tc}$ : 16.119       $b_{Tc}$ : 8.0586  
 $a_1$ : 0.059829       $a_2$ : 0.001028

- **Stripping correction (IAEA, 2003)**

#### 2012 survey data

Used parameters (determined from measurements on calibrations pads at the NGU and Borlänge airport):

a 0.04840  
b -0.00121  
g -0.00074  
alpha 0.29993  
beta 0.47548

gamma 0.83135

### **2013 survey data**

Used parameters (determined from measurements on calibrations pads at the NGU on May 6 2013):

a 0.049524  
b -0.00169  
g -0.00131  
alpha 0.29698  
beta 0.47138  
gamma 0.82905

### **2014 survey data**

Used parameters (determined from measurements on calibrations pads at the NGU on June 5 2014):

a 0.047186  
b -0.00166  
g -0.00145  
alpha 0.305607  
beta 0.484063  
gamma 0.814612

- **Height correction to a height of 60 m**

#### **2012 survey data**

Used parameters (determined by height calibration flight at near Seljord in June 2012):

Attenuation factors in 1/m:

K: -0.0072  
U: -0.0058  
Th: -0.0058  
Total counts: -0.0056

#### **2013 survey data**

Used parameters (determined by high altitude calibration flights near near Frosta in January 2014):

Attenuation factors in 1/m:

K: -0.00888  
U: -0.00653  
Th: -0.00662  
TC: -0.00773

#### **2014 survey data**

Used parameters (determined by high altitude calibration flights near near Frosta in January 2014):

Attenuation factors in 1/m:

K: -0.009523  
U: -0.006687  
Th: -0.007393  
TC: -0.00773

- **Converting counts at 60 m heights to element concentration on the ground**

#### **2012 survey data**

Used parameters (determined from measurements on calibrations pads at the NGU and Borlänge airport):

Counts per elements concentrations:

K: 0.00757 %/counts  
U: 0.087834 ppm/counts  
Th: 0.154092 ppm/counts

#### **2013 survey data**

Used parameters (determined from measurements on calibrations pads at the NGU on May 6 2013):

Sensitivity (elements concentrations per count)::

K: 0.007545 %/counts  
U: 0.088909 ppm/counts  
Th: 0.151433 ppm/counts

### **2014 survey data**

Used parameters (determined from measurements on calibrations pads at the NGU on May 6 2013):

Sensitivity (elements concentrations per count)::

K: 0.007480 %/counts  
U: 0.087599 ppm/counts  
Th: 0.156147 ppm/counts

- **Microlevelling using Geosoft menu and smoothing by a convolution filtering**

Used parameters for microlevelling:

De-corrugation cutoff wavelength:	800 m
Cell size for gridding:	200 m
Naudy (1968) Filter length:	800 m

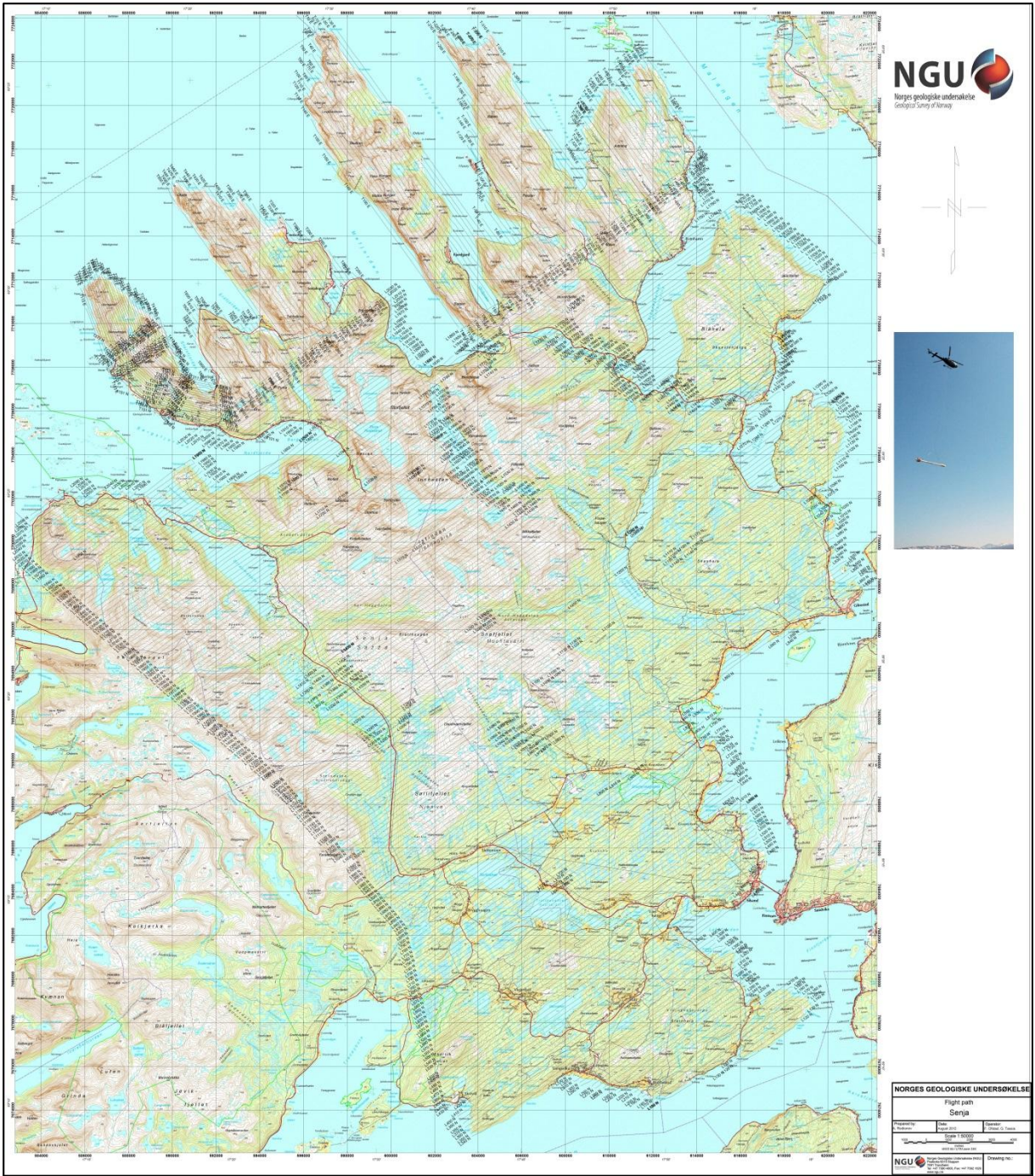


Figure 4: Senja survey area with flight path

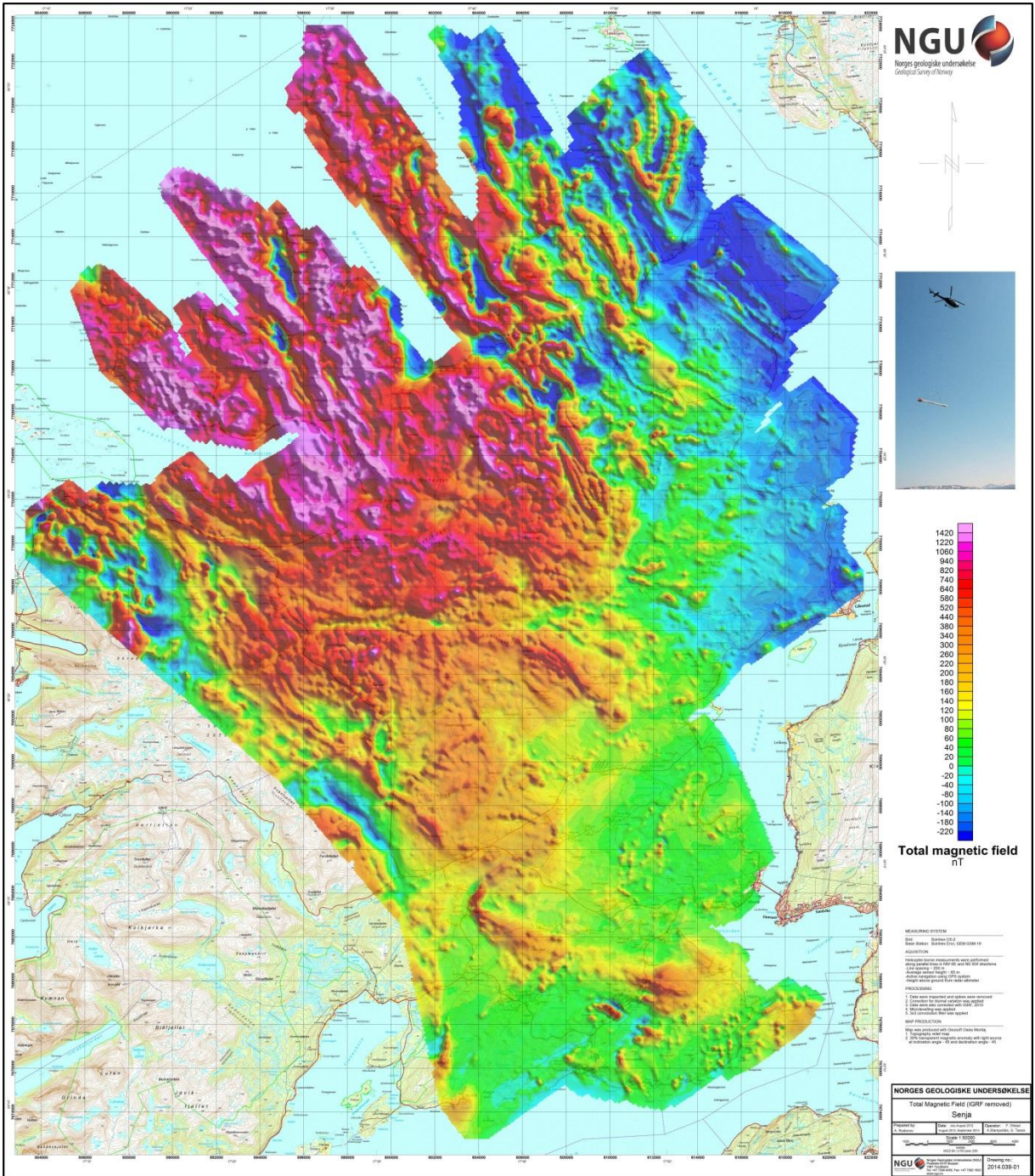


Figure 5: Total Magnetic Field

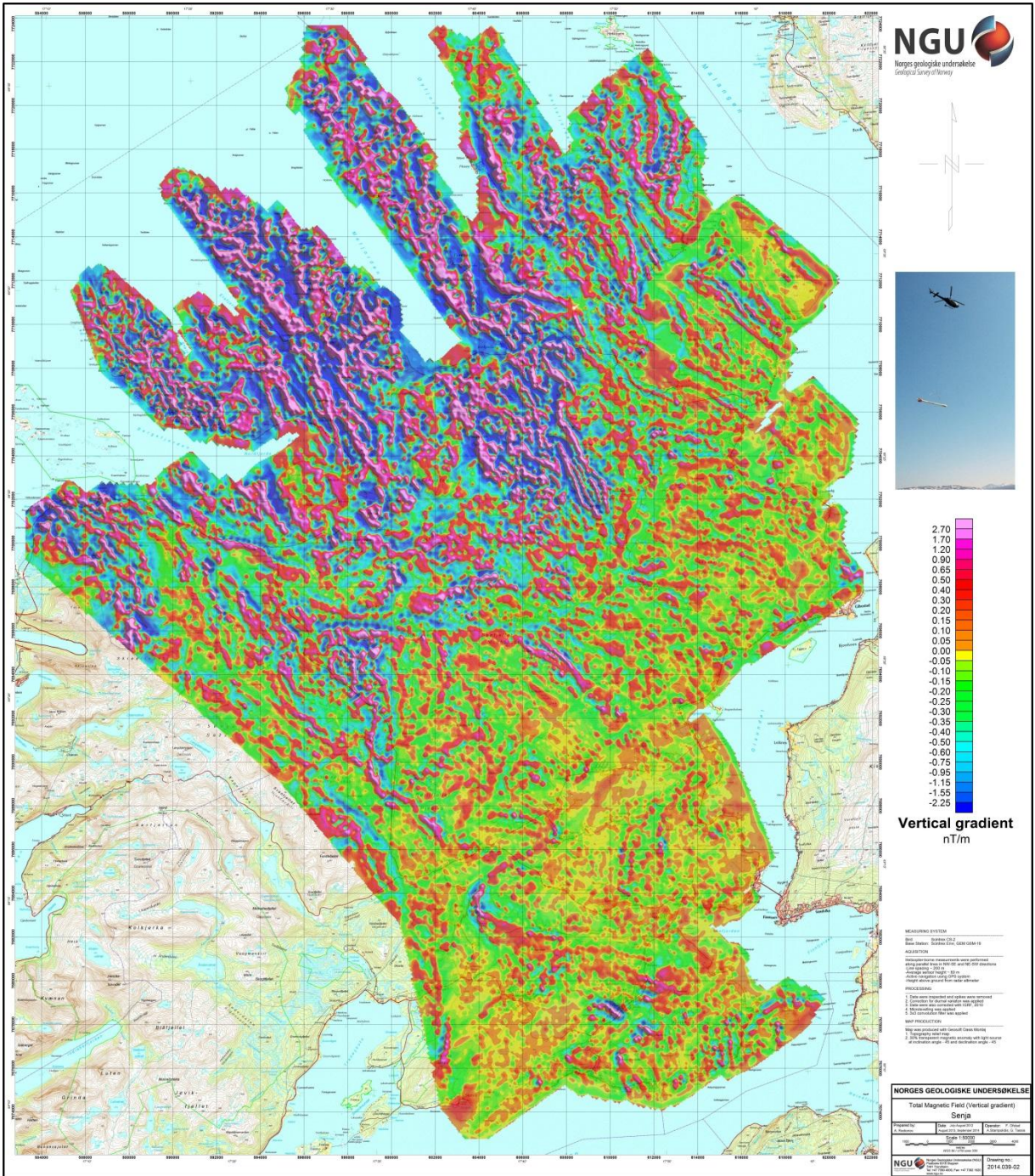


Figure 6: Magnetic Vertical Derivative

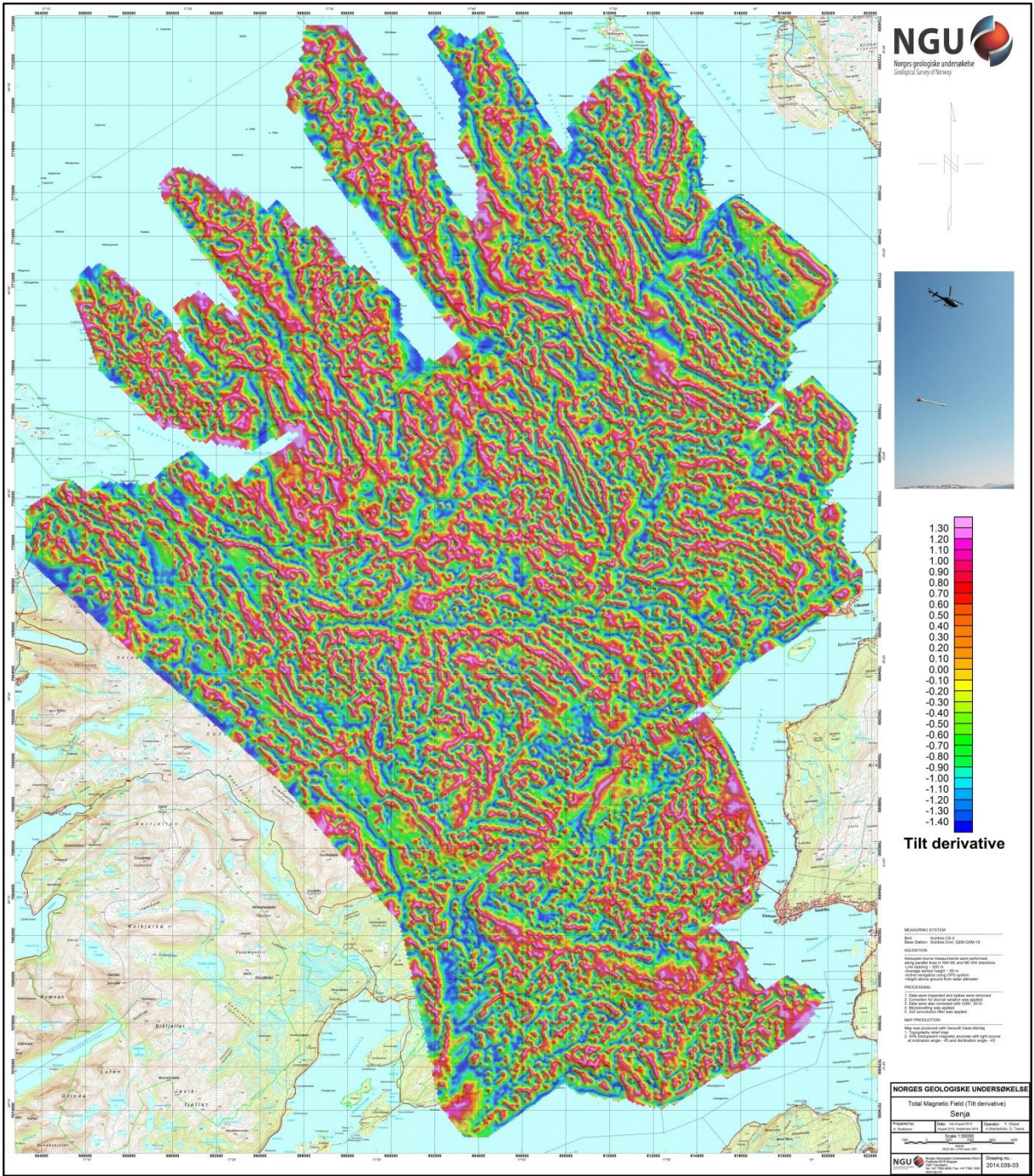


Figure 7: Magnetic Tilt Derivative

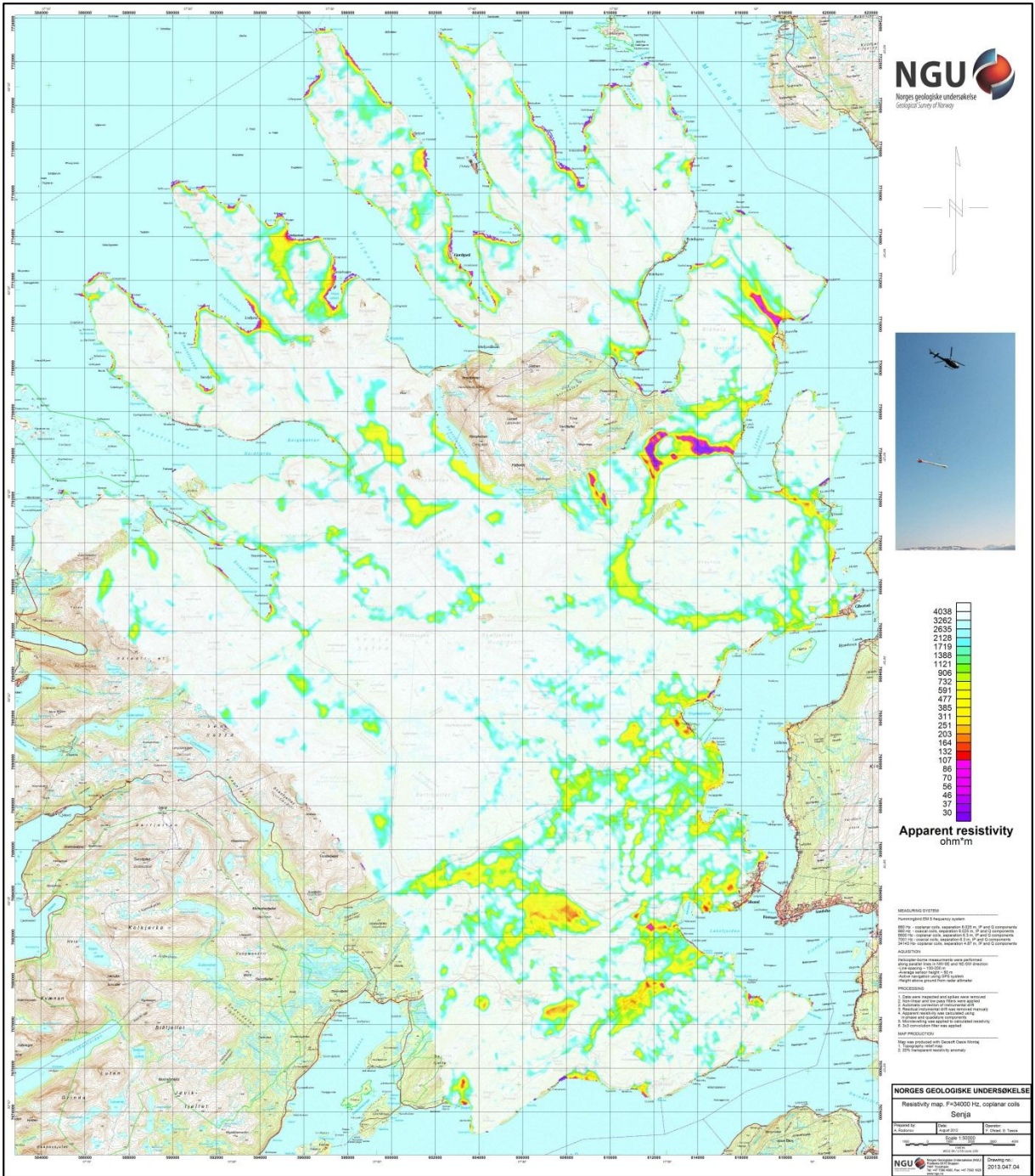


Figure 8: Apparent resistivity. Frequency 34000 Hz, Coplanar coils

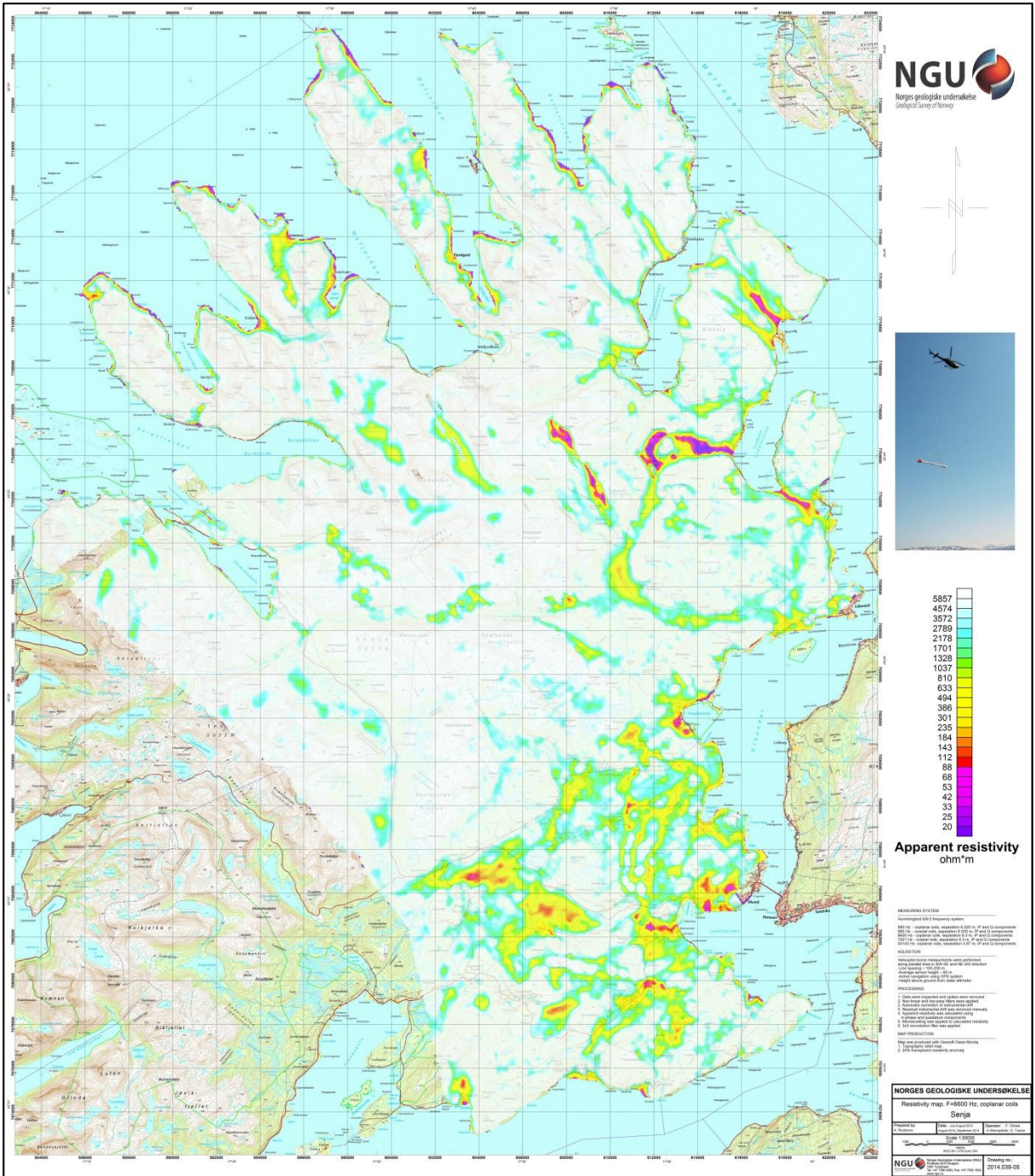


Figure 9: Apparent resistivity. Frequency 6600 Hz, Coplanar coils

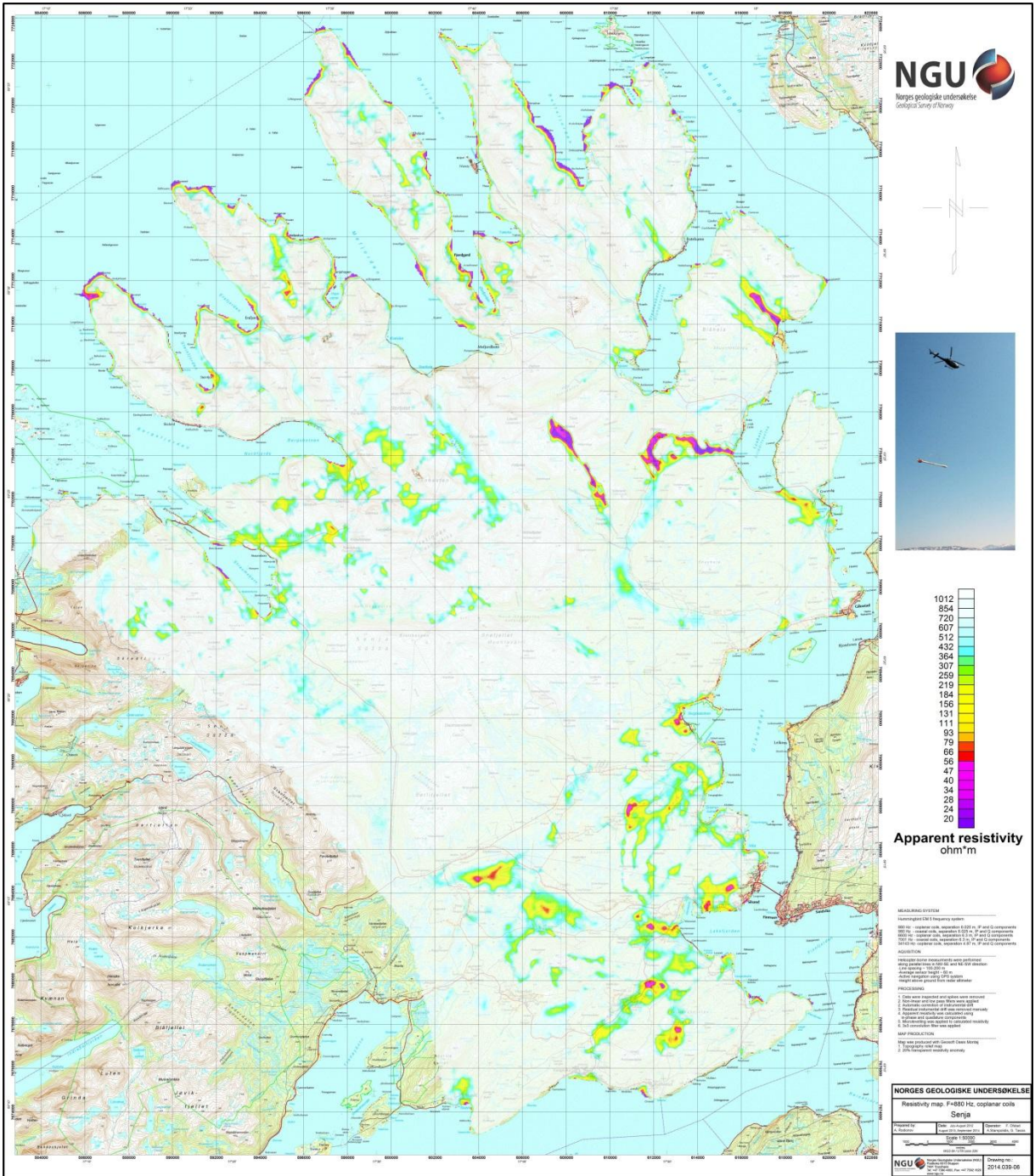


Figure 10: Apparent resistivity. Frequency 880 Hz, coplanar coils

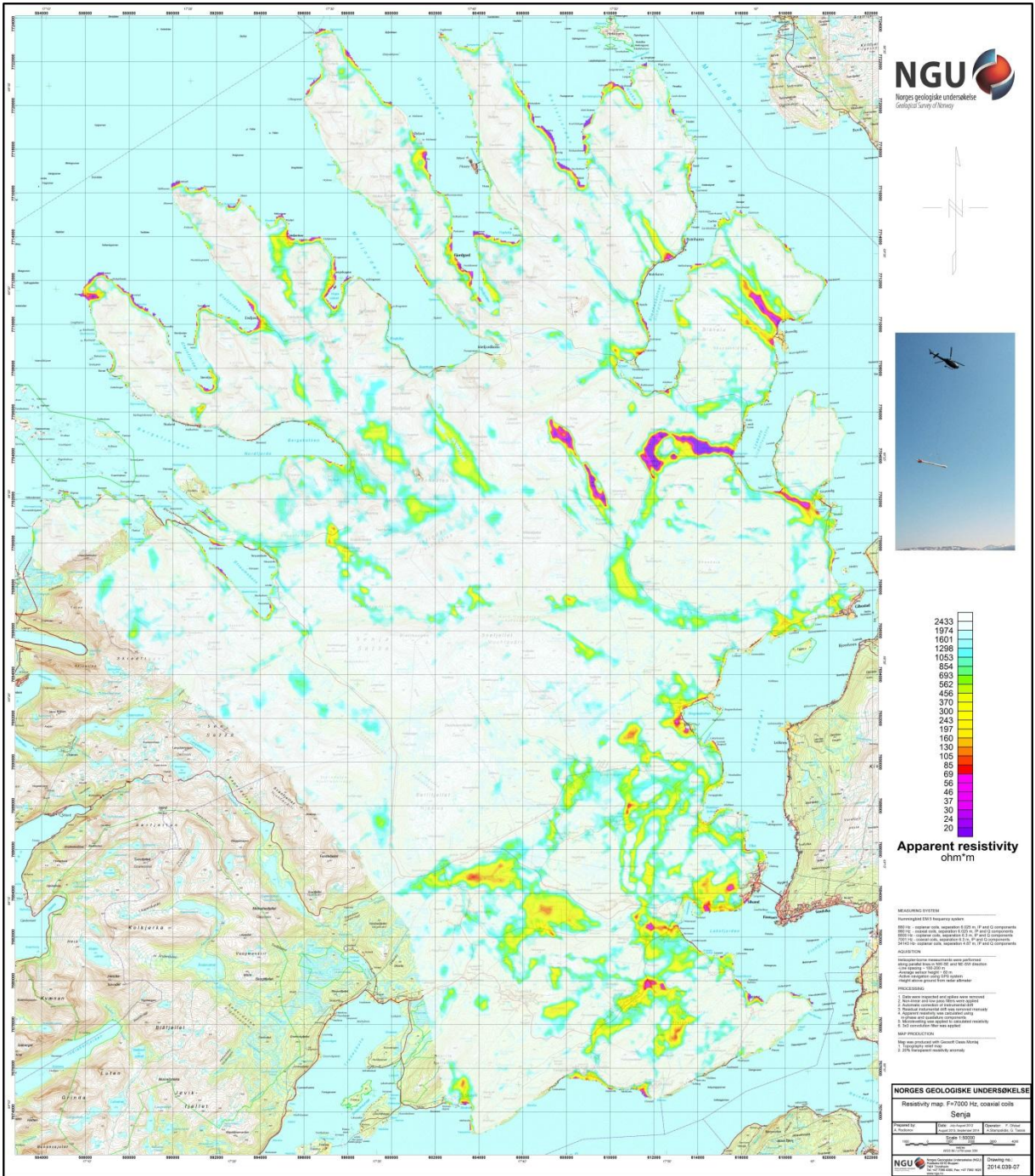


Figure 11: Apparent resistivity. Frequency 7000 Hz, Coaxial coils

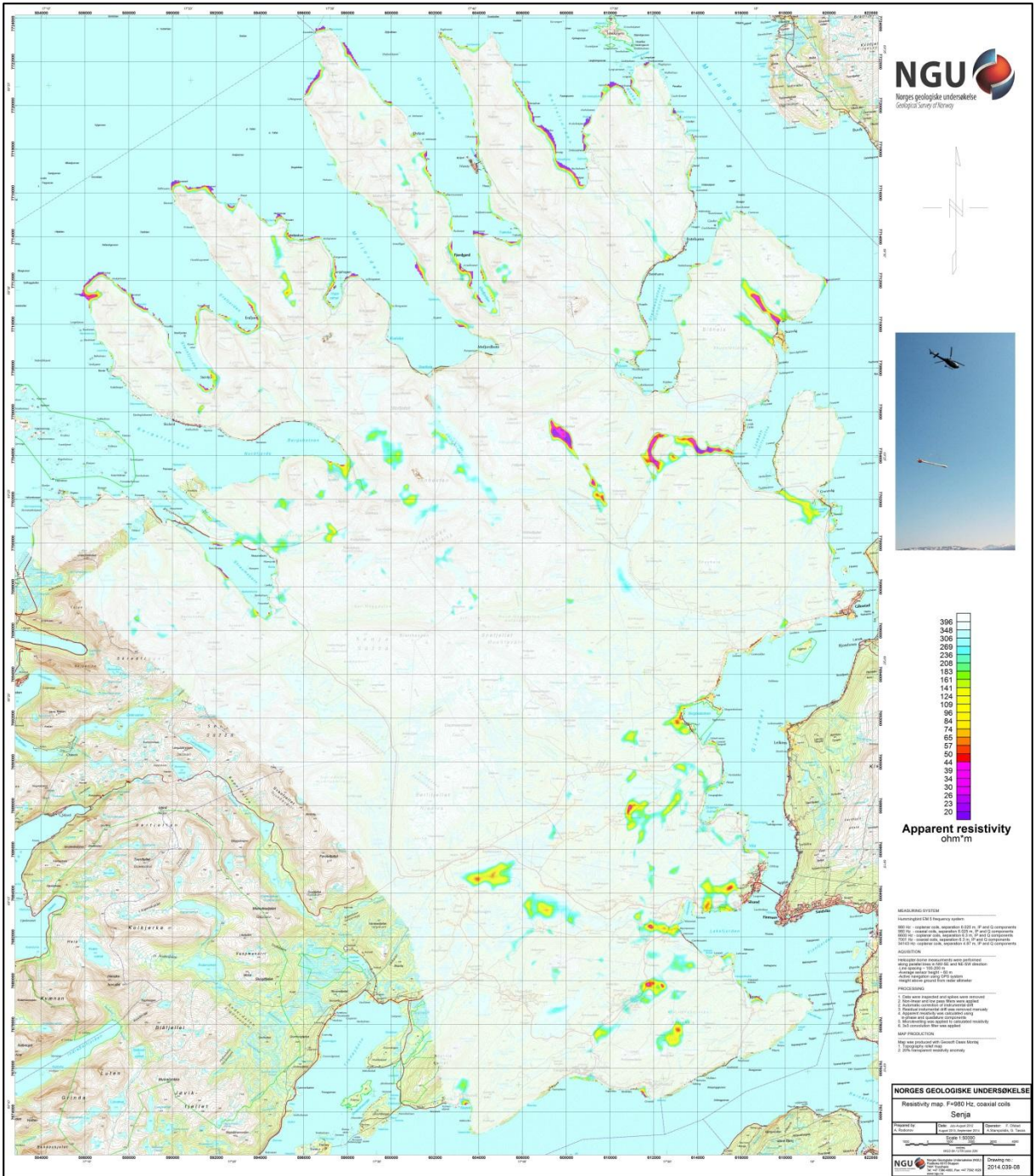


Figure 12: In-phase and quadrature responses. Frequency 980 Hz, Coaxial coils

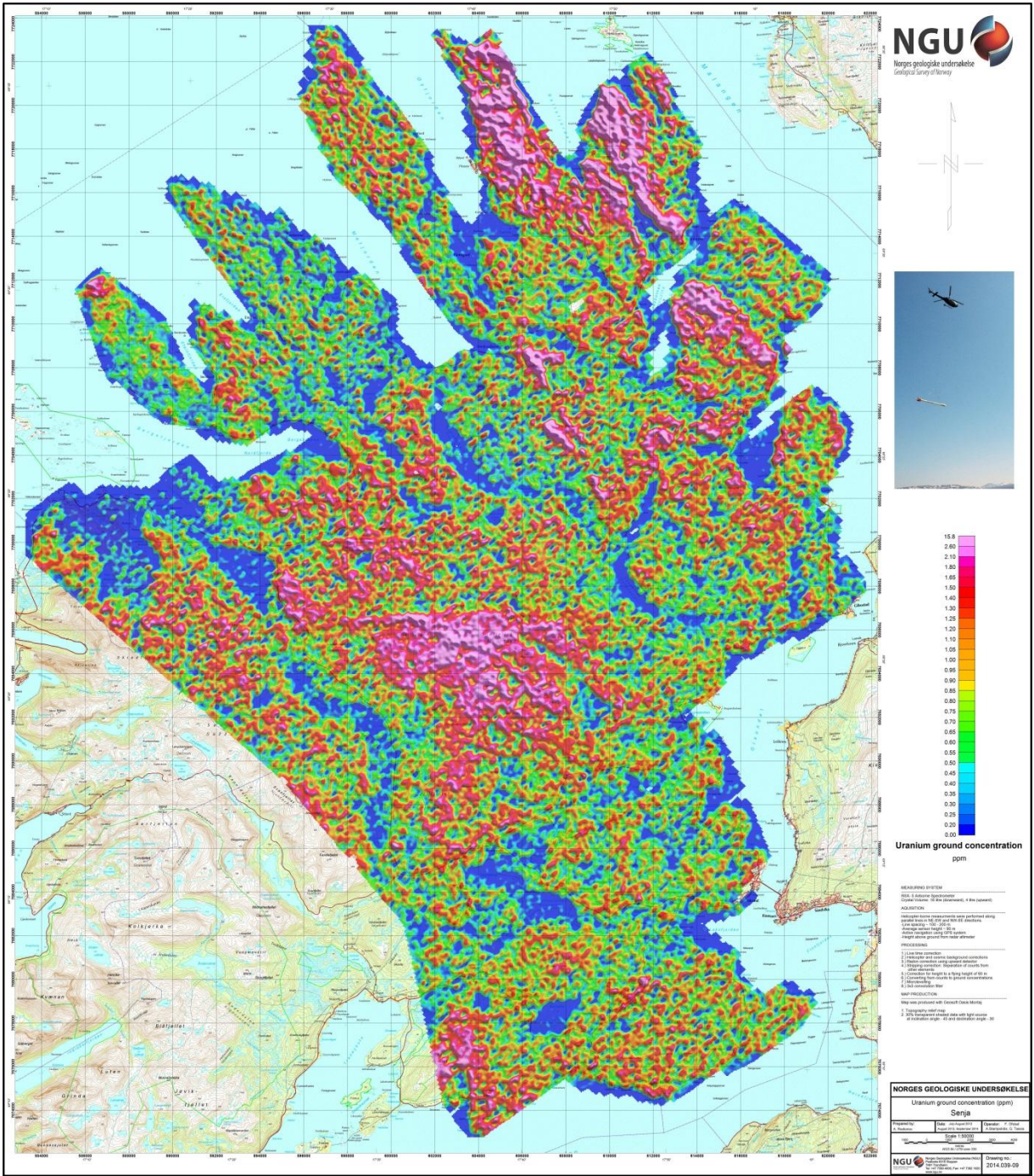


Figure 13: Uranium ground concentration

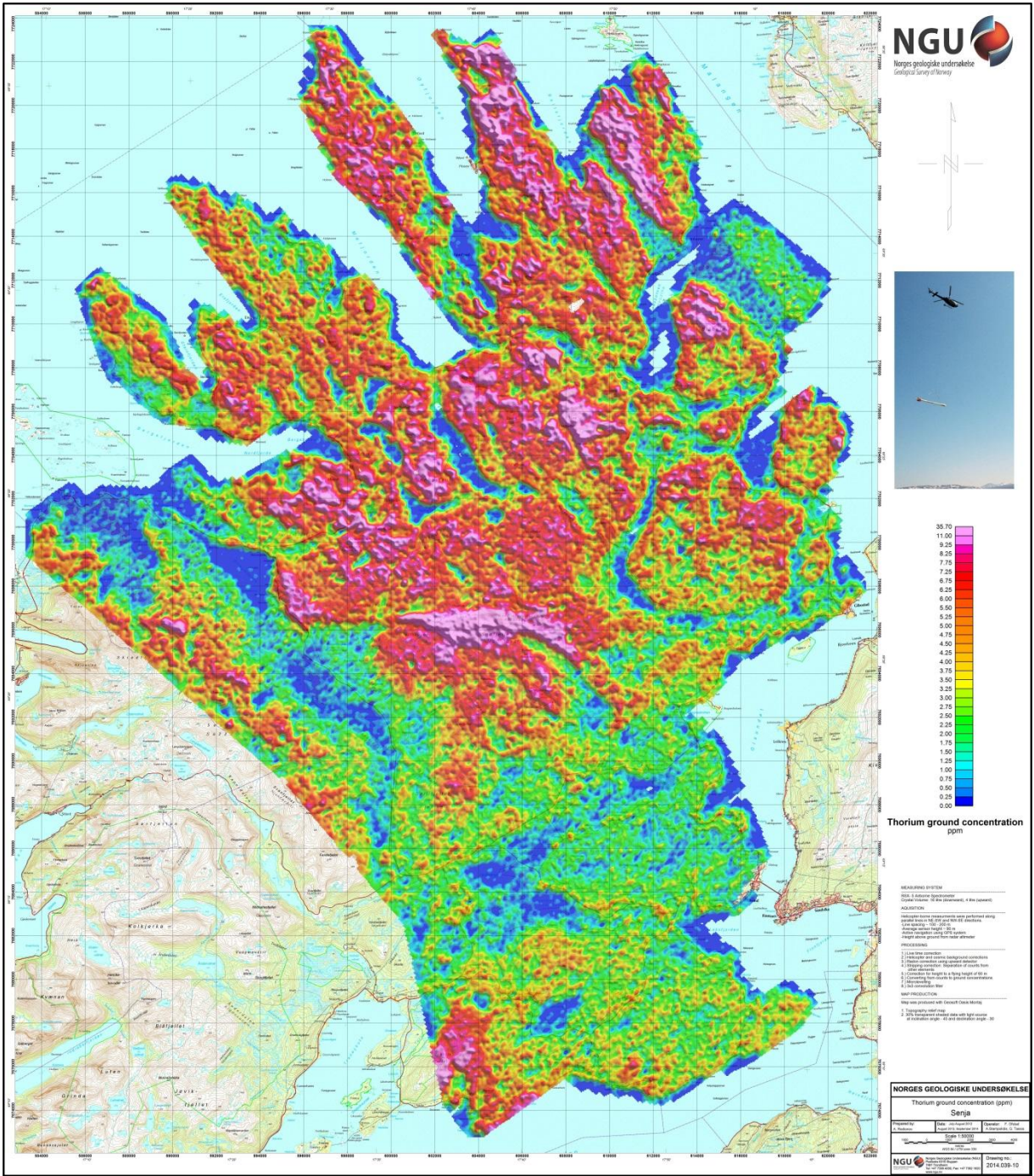


Figure 14: Thorium ground concentration

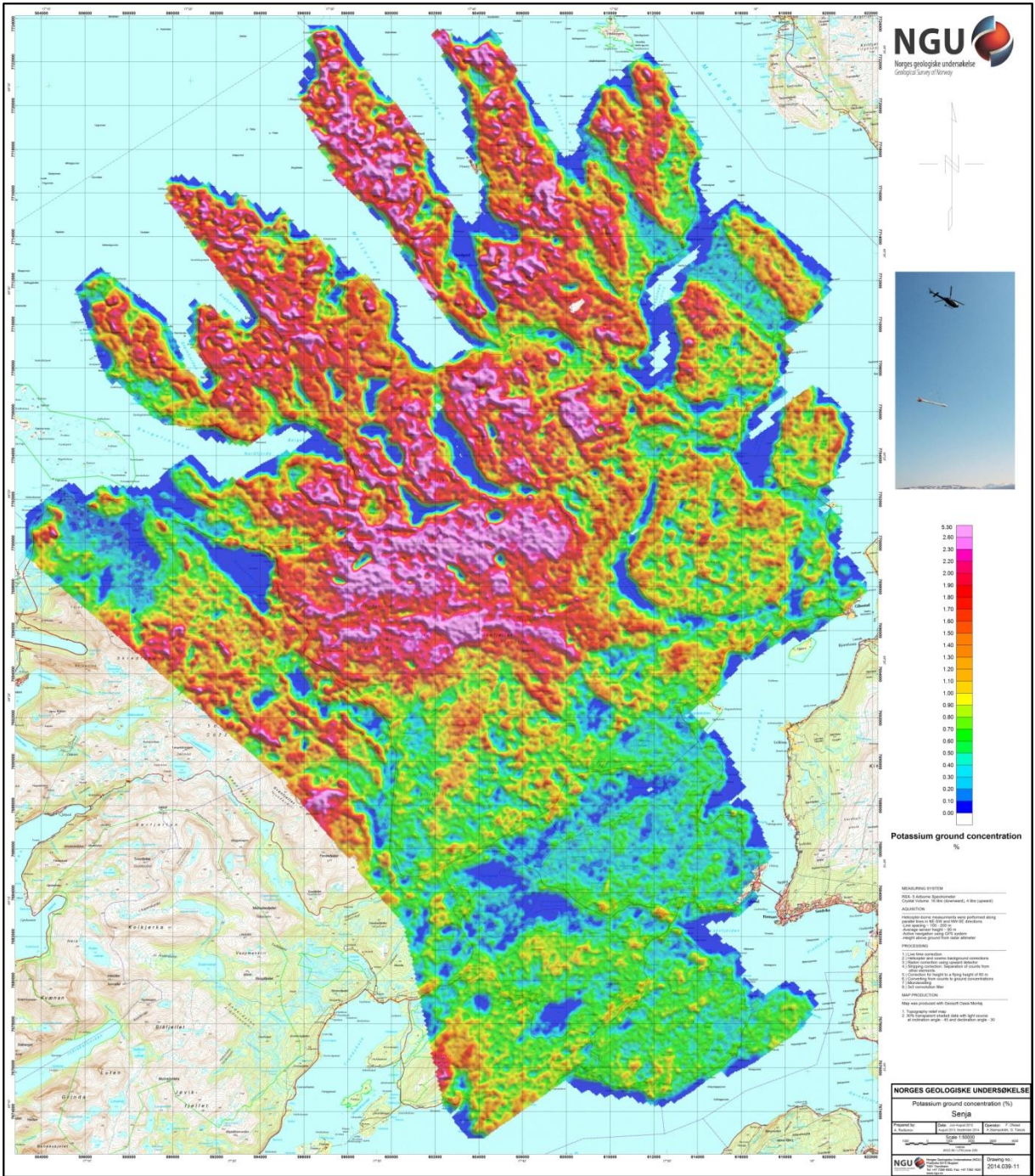


Figure 15: Potassium ground concentration

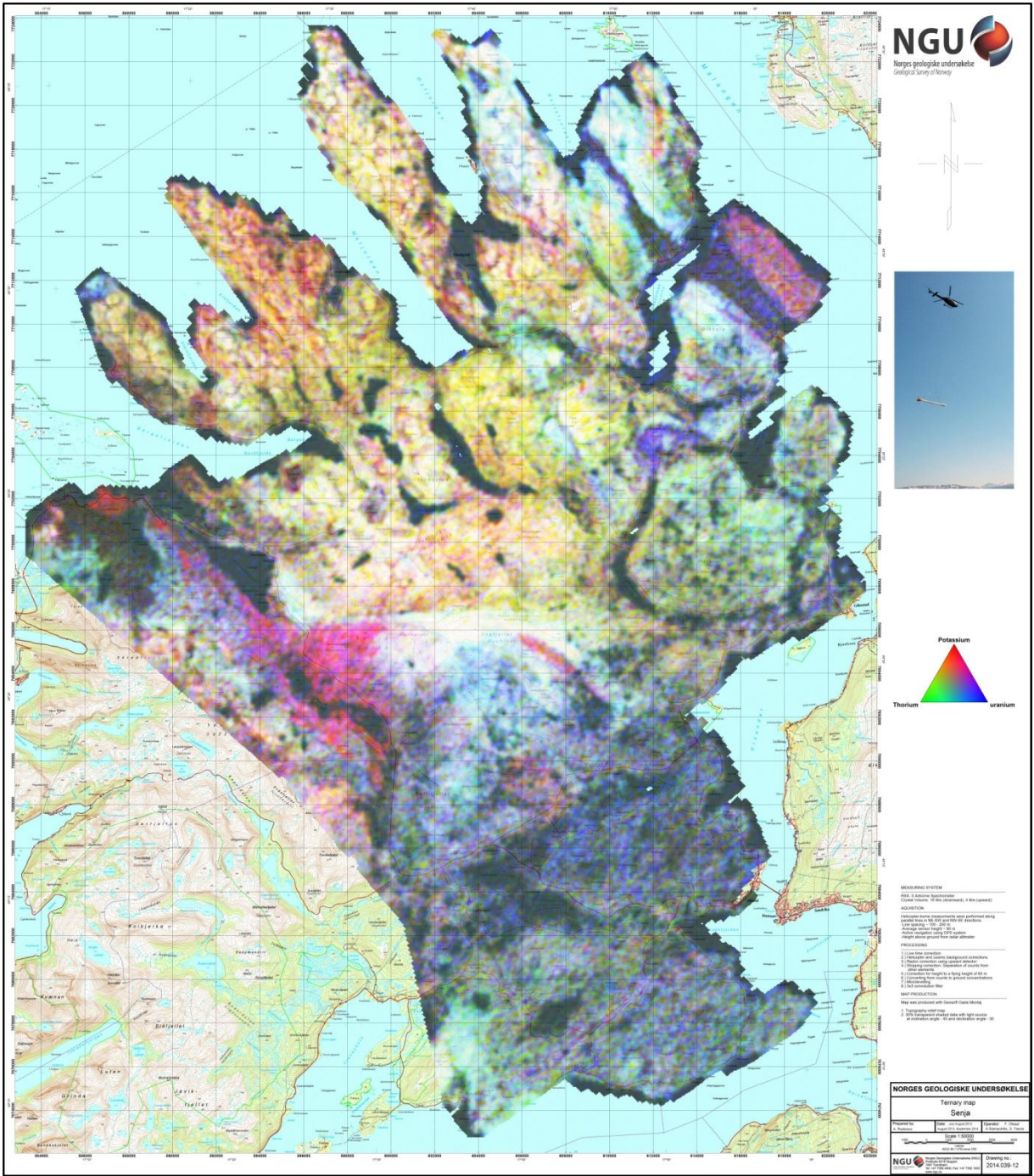


Figure 16: Radiometric Ternary map